Advanced Composite Materials
Publication details, including instructions for authors and subscription information:
http://www.tandfonline.com/loi/tacm20

Progressive failure of laminated composites with a hole under compressive loading based on micro-mechanics

Wangnan Li[a], Hongneng Cai[a], Chao Li[a], Kaixin Wang[a] & Liang Fang[a]
[a] State Key Laboratory for Mechanical Behavior of Materials, Xi'an Jiaotong University, 28, West Xianning Road, Xi'an, Shaanxi 710049, P.R. China
Published online: 01 Aug 2014.

To cite this article: Wangnan Li, Hongneng Cai, Chao Li, Kaixin Wang & Liang Fang (2014) Progressive failure of laminated composites with a hole under compressive loading based on micro-mechanics, Advanced Composite Materials, 23:5-6, 477-490, DOI: 10.1080/09243046.2014.915105

To link to this article: http://dx.doi.org/10.1080/09243046.2014.915105

Advanced Composite Materials, 2014
Vol. 23, Nos. 5–6, 477–490, http://dx.doi.org/10.1080/09243046.2014.915105

Progressive failure of laminated composites with a hole under compressive loading based on micro-mechanics

Wangnan Li, Hongneng Cai*, Chao Li, Kaixin Wang and Liang Fang

State Key Laboratory for Mechanical Behavior of Materials, Xi'an Jiaotong University, 28, West Xianning Road, Xi'an, Shaanxi 710049, P.R. China

(*Received 7 January 2014; accepted 24 March 2014*)

This paper deals with progressive failure analysis of composites structure on the basis of the theory of micro-mechanics of failure (MMF). The MMF theory includes micro-scale stress amplification within each constituent material (fiber and matrix) and failure criteria for the judgment of the constituent failure. The unit cell model with the face-centered array distribution of carbon fibers is constructed to analyze the micro-scale stress amplification factors in the fiber and matrix. Noninteractive failure criteria are proposed to judge the failure of the fiber and matrix. During the process of loading, the constituents' failure can be identified by the MMF failure criteria, and then the material properties degradation scheme is evaluated according to the failure modes of constituents and applied for each element to continue the progressive failure analysis for the composite materials. The user-defined material subroutine for the micro-scale stress amplification in the constituents, failure judgment of the constituents, and degradation of ply properties is developed using the Abaqus Fortran scripts. Micro-scale stress of the constituents is visualized for detailed analysis. The initial failure, subsequent propagation, final failure, and the strength of open-hole compression (OHC) structure of the carbon fiber-reinforced polymer composites are studied based on MMF theory. The ultimate load and failure behavior of the OHC structure obtained from both theoretical analysis and tests are compared and analyzed.

Keywords: micro-mechanics of failure; noninteractive failure criteria; micro-scale stress; UMAT; progressive failure

1. Introduction

In recent years, composite materials are used in various advanced structures and other relevant fields due to their high specific strength and stiffness, outstanding design ability, long fatigue life, corrosive resistance. Whether or not the composite material can be used widely in the engineering application depends on that the strength of the composite structure can be correctly evaluated at various loading condition. The strength prediction and progressive failure analysis for composite materials have attracted many researchers' attention.[1–6] In the process of numerical simulation of composite laminates stress field, the macroscopic lamina-based strength theories for composite material are widely used because they are simple, easy to be understood, and implemented in analysis,[7–9] but the specific failure mechanism is not indicated when the conventional strength theories were used for practical design. In addition, those theories are essentially used for the

*Corresponding author. Email: hntsai@mail.xjtu.edu.cn

two-dimensional cases, where the thickness effect is ignored, so the classical plate and shell-based laminate strength theories are not adequate for the three-dimensional stress analysis for the large structures with thick and curved characters. Moreover, the classical theories were established using the mathematics approximation formulas which satisfy some key points given by experimental result. Large error occurs during prediction of strength of the structure under complicated loading conditions. Because of the limitation of macroscopic failure criteria, the scientists suggest a more reliable strength theory for composite materials should be developed.

Recently, the quasi-physically based failure theories have been used to analyze ultimate load and failure behavior of the composite structure which have separate predictions of fiber-dominated and matrix-dominated failures.[1,10–12] Hashin's [13] and Puck's [14] theories fall into this category and partly account for their popularity in progressive failure modeling, but those theories cannot point out the micro-scale stress of the constituents.

The micro-mechanics of failure (MMF) proposed by Ha [15] is a real physics-based strength theory for strength prediction of the structures made of carbon fiber-reinforced polymer (CFRP) laminates, in which the initial failure of constituents is analyzed in micro-level with the interactive failure criteria. In their research, the square or hexagonal unit cell model applied with the loads, corresponding to the stress state in macro-level, at the boundaries was used to look into the stresses in fibers and matrix in micro-level. Based on the interactive MMF, both transverse tensile and compressive failure of the Graphite/Epoxy were analyzed in that paper. In this way, the strength and failure modes of laminate with multidirectional stacking sequence have been predicted. These predictions are compared with predictions from other widely used failure criteria as well as experimental data, good agreement was confirmed. However, the large amount of iterative calculation for the extraction of the MMF critical parameters using the interactive failure criteria lowers the computational efficiency and has a poor convergence performance. Therefore, a simple and reliable MMF failure criterion that can increase computational efficiency and improve the convergence is necessary.

The MMF theory was extended to analyze stresses of the three-dimensional structures made of CFRP laminates by the authors [16] with the noninteractive MMF failure criteria and the unit cell model with the face-centered array distribution of carbon fibers. The study gave out an accurate initial strength prediction for the open-hole compression (OHC) structures of polymer composites. The method was established using the Abaqus Python scripts and user-defined material subroutine (UMAT) written in Fortran scripts. The UMAT was used to convert the stress in macro-level to the stresses in the key points in the fiber and matrix in micro-level. The mechanical properties of fiber were calculated using the mixture rules.

In this paper, progressive failure analysis method based on the MMF theory for the prediction of the ultimate load of the CFRP laminate structures is developed. In order to improve the analysis accuracy, the finite element analysis and artificial neural networks are used to back-calculate the transverse Young's modulus of the fiber E_{f2} and shear modulus of the fiber G_{f12}. Also, the nonlinear shear behavior of laminate is taken into account. During each step of loading, the constituents' failure is identified by the noninteractive MMF failure criteria, and then the material properties degradation scheme is evaluated according to the failure modes of constituents and applied for each element for the subsequence failure analysis. The new UMAT for the micro-scale stress amplification in constituents, failure judgment of the constituents and properties degradation of the plies are developed using the Abaqus Fortran scripts. Micro-scale stress of the constituents is visualized for detailed analysis. The ultimate load and the failure behavior of the OHC structure are studied based on MMF theory.

2. The micro-mechanics-based strength theory for composites

2.1. MMF criteria

The composite material is characterized using four MMF critical parameters, including the tensile strength of fibers T_f, the compressive strength of fibers C_f, the tensile strength of matrix T_m, and the compressive strength of matrix C_m. T_f and C_f are used to judge the failure of fibers under tensile and compressive loading, respectively. T_m and C_m are used to judge the failure of matrix under tensile and compressive loading, respectively. The computing methods of the MMF critical parameters are shown in Equation (1),

$$\begin{cases} T_f = \sigma_1^f, & (\sigma_1^f > 0) \\ C_f = \sigma_{eq}^f, & (\sigma_1^f < 0) \\ T_m = I_1^m \\ C_m = \sigma_{eq}^m \end{cases} \quad (1)$$

where T_f and C_f are extracted using the maximum stress in fiber direction, and T_m and C_m are extracted using the function of stress components at the key points of matrix. The material axes 123 are used as coordinate direction. The σ_1 is the stress of fiber direction, I_1 is the first stress invariant, and σ_{eq} is the equivalent stress. The superscript and subscript, f and m, represent the fiber and matrix, respectively.

Here, it may be pointed out that Christensen [17] proposed the interactive failure criteria to judge the failure of the matrix, however, the extraction of T_m and C_m from the results of the unidirectional laminate tests is very difficult for the engineering application because of the complexity to extract the critical parameters of the constituents from the test results for the unidirectional laminates. Therefore, the simple and noninteractive failure criteria for the matrix are proposed to judge the failure. When the maximal first stress invariant I_1 in the matrix of the element reaches T_m, or the maximum equivalent stress in the matrix of the element reaches C_m, the crack will occur in the matrix. The noninteractive failure criteria are easy to be applied in practical engineering.

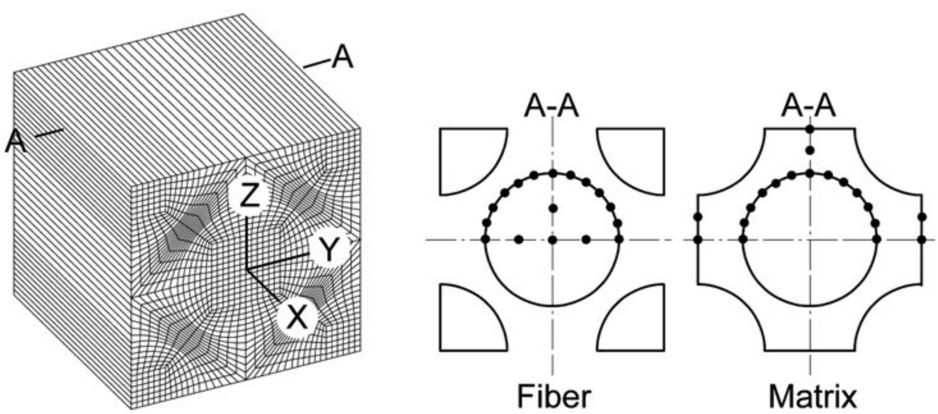

Figure 1. The unit cell model with the face-centered array distribution of carbon fibers and location of key points for the extraction of stress amplification factors within unit cell.

2.2. Unit cell model for micro-mechanics analysis

The micro-scale stresses amplification in fiber and matrix can be analyzed using unit cell model. Two typical unit cell models, i.e. square model and hexagonal model are used in the micro-scale stresses amplification factors analysis. Compared with the square model, the hexagonal model includes more fibers and can reflect the interactive effect between the fibers. The result of the research shows that the strength prediction using the hexagonal model agrees well with the test data.[15] But the hexagonal model cannot explain the 'homogeneous' characteristics in the transverse y and z directions of material coordinate in the macro-level due to the length difference between the edges of hexagonal unit cell model in the y and z directions. Therefore, the unit cell model with the face-centered array distribution of carbon fibers is constructed to analyze the stresses amplification in fibers and matrix in micro-level as shown in Figure 1, whereby individual fiber and matrix are modeled by three-dimensional elements. This unit cell model is applied with prescribed loads of average unit stress in one of three normal stresses or one of three shear stresses as well as thermal load with temperature increment one degree. The boundary constraint conditions set for the model are same as described in the literature by Cai et al. [18].

The local stresses are extracted from various positions in the representative micro-mechanical unit cell model, 17 key points in fiber and 19 key points in matrix. The extracted stresses are normalized as mechanical amplification factors of the stresses in the lamina at macro-level. One input stress in macro-level in lamina maps 36 sets of states of stresses, i.e. 17 sets for fiber and 19 sets for matrix, and stored as micro-scale stress amplification factors. The normalized thermal residual stresses are also considered as thermal-mechanical amplification factors. The thermal residual stresses occur from the temperature difference from the curing temperature to room temperature.

The macro-stresses of lamina are converted into the stresses of fiber and matrix in micro-level using the stress amplification factors. The output result of macro-stresses from the finite element analysis at macro-level or from classical laminated plate criteria is amplified through these amplification factors before failure analysis. The critical point among these key points is identified by comparing the values of strength ratio using failure criteria with the MMF critical parameters of the constituents. The stresses modification from the macro-level to the micro-level is carried out with the expression using the obtained stress amplification factors as follows:

$$\begin{pmatrix} \sigma_1 \\ \sigma_2 \\ \sigma_3 \\ \tau_{12} \\ \tau_{13} \\ \tau_{23} \end{pmatrix}^{(i)}_{\text{mech}} = \begin{bmatrix} M11 & M12 & M13 & M14 & M15 & M16 \\ M21 & M22 & M23 & M24 & M25 & M26 \\ M31 & M32 & M33 & M34 & M35 & M36 \\ M41 & M42 & M43 & M44 & M45 & M46 \\ M51 & M52 & M53 & M54 & M55 & M56 \\ M61 & M62 & M63 & M64 & M65 & M66 \end{bmatrix}^{(i)}_{\sigma} \begin{pmatrix} \overline{\sigma}_1 \\ \overline{\sigma}_2 \\ \overline{\sigma}_3 \\ \overline{\tau}_{12} \\ \overline{\tau}_{13} \\ \overline{\tau}_{23} \end{pmatrix}_{\text{mech}} + \begin{pmatrix} A1 \\ A2 \\ A3 \\ A4 \\ A5 \\ A6 \end{pmatrix}^{(i)}_{\sigma} \Delta T \tag{2}$$

where $\sigma^{(i)}_{\text{mech}}$ is the micro-stress of the key pint i in fiber or matrix, $\overline{\sigma}_{\text{mech}}$ is the macro-stress in CFRP lamina, ΔT is the temperature difference between environment temperature and the curing temperature, $M^{(i)}_{\sigma}$ is the stress amplification factors of the key point i either in fiber or matrix resin, and $A^{(i)}_{\sigma}$ is the thermal stress amplification factors for the key point i.

2.3. Extraction of the MMF critical parameters

In the MMF theory, the MMF critical parameters, T_f, C_f, T_m, and C_m can be extracted from the laminate strengths with the unit cell model and key points. The strengths of fiber can be calculated, using the stress amplification factors of key points in fiber, and the UD laminate longitudinal tensile strength X and compressive strength X', respectively. The $\sigma_1^{f,i}$ of key points is taken as MMF parameters of fibers where longitudinal tensile stress exists. The maximum $\sigma_1^{f,i}$among these key points is extracted and symbolized as T_f. Similarly, the $\sigma_{eq}^{f,i}$ of key points is taken as MMF parameters of fibers where longitudinal compressive stress exists. The maximum $\sigma_{eq}^{f,i}$ among these key points is taken as C_f. The superscript number i is the key point number in the fiber from 1 to 17.

The strengths of matrix can be extracted using the stress amplification factors of key points in matrix, and the UD laminate transverse tensile strength Y and compressive strength Y', respectively. The first invariant of stress $I_1^{m,j}$ of these key points is taken as MMF parameters of matrix where volumetric dilatation exists. The maximum $I_1^{m,j}$ among these key points is extracted and taken as T_m. The equivalent stress $\sigma_{eq}^{m,j}$ of key points is taken as MMF parameters of matrix where compressive stress exists. The maximum $\sigma_{eq}^{m,j}$ among these key points is taken as C_m. The superscript number j is the key point number in the matrix from 1 to 19.

2.4. Failure indices of the constituents

The general failure index k of ply depends on the four specific failure indices of the constituents which correspond to the different failure modes. At a material point, failure is deemed to occur when the failure indices k reaches 1 with the failure mode being identified by whichever failure criterion is satisfied first. The failure indices of the constituents are defined as:

$$\begin{aligned} k &= \max[k_{T,f}, k_{C,f}, k_{T,m}, k_{C,m}] \\ k_{T,f} &= \max(\sigma_1^{f,1}/T_f, \ldots, \sigma_1^{f,i}/T_f, \ldots, \sigma_1^{f,n_1}/T_f) \\ k_{C,f} &= \max(\sigma_{eq}^{f,1}/C_f, \ldots, \sigma_{eq}^{f,i}/C_f, \ldots, \sigma_{eq}^{f,n_1}/C_f) \\ k_{T,m} &= \max(I_1^{m,1}/T_m, \ldots, I_1^{m,j}/T_m, \ldots, I_1^{m,n_2}/T_m) \\ k_{C,m} &= \max(\sigma_{eq}^{m,1}/C_m, \ldots, \sigma_{eq}^{m,j}/C_m, \ldots, \sigma_{eq}^{m,n_2}/C_m) \end{aligned} \tag{3}$$

where k without subscript means the failure index of the element; $k_{T,\ f}$ and $k_{C,\ f}$ are the fiber tensile failure index and fiber compressive failure index; $k_{T,\ m}$ and $k_{C,\ m}$ are the matrix tensile failure index and matrix compressive failure index; $i = 1 \ldots n_1$, $j = 1 \ldots n_2$, n_1, n_2 represent the total numbers of the key points in the fiber and matrix, respectively.

3. Damage model derivation

Damage plays an important role in the analysis of fiber-reinforced composite materials. Many such materials exhibit elastic-brittle behavior; that is, damage in these materials is initiated without significant plastic deformation. Consequently, plasticity can be neglected when modeling the behavior of such materials.

The effect of damage can be taken into account by reducing the values of stiffness coefficients as originally proposed by Kachanov [19]. Here we adapt the model formulated by McCarthy et al. [20] to compute the degradation of coefficients of the stiffness matrix and the nonlinear model used by Li et al. [16] to input the nonlinear shear behavior of the laminate. In the damage model, the material stiffness matrix $[C]_{ijkl}$ is established as follow:

$$[C]_{ijkl} = \begin{bmatrix} C_{11} & C_{12} & C_{13} & 0 & 0 & 0 \\ & C_{22} & C_{23} & 0 & 0 & 0 \\ & & C_{33} & 0 & 0 & 0 \\ & \text{symm} & & C_{44} & 0 & 0 \\ & & & & C_{55} & 0 \\ & & & & & C_{66} \end{bmatrix} \tag{4}$$

where

$$\begin{aligned} C_{11} &= E_1(1-d_f)[1-(1-d_m)^2 v_{23}^2]/A \\ C_{22} &= E_2(1-d_m)[1-(1-d_m)(1-d_f)v_{13}v_{31}]/A \\ C_{33} &= E_2(1-d_m)[1-(1-d_m)(1-d_f)v_{12}v_{21}]/A \\ C_{12} &= E_2(1-d_m)(1-d_f)[(1-d_m)v_{13}v_{23}+v_{12}]/A \\ C_{13} &= E_2(1-d_m)(1-d_f)[(1-d_m)v_{12}v_{23}+v_{13}]/A \\ C_{23} &= E_2(1-d_m)^2[v_{23}^2+(1-d_f)v_{12}v_{31}]/A \\ C_{44} &= G_{12}(1-d_m)(1-d_f) \\ C_{55} &= G_{13}(1-d_m)(1-d_f) \\ C_{66} &= G_{23}(1-d_m)(1-d_f) \end{aligned} \tag{5}$$

$$\begin{aligned} A = 1 &- (1-d_m)(1-d_f)v_{12}v_{21} - (1-d_m)^2 v_{23}v_{32} \\ &-(1-d_m)(1-d_f)v_{13}v_{31} - 2(1-d_m)^2(1-d_f)v_{12}v_{31}v_{23} \end{aligned}$$

where d_f is the fiber damage parameter; d_m is the matrix damage parameter. The d_f and d_m are described below,

Tensile fiber failure ($\sigma_1^f > 0$)

$$\text{If } k_{T,f} \geq 1, \text{ then } d_f = 0.99 \tag{6}$$

Compressive fiber failure ($\sigma_1^f < 0$)

$$\text{If } k_{C,f} \geq 1, \text{ then } d_f = 0.99 \tag{7}$$

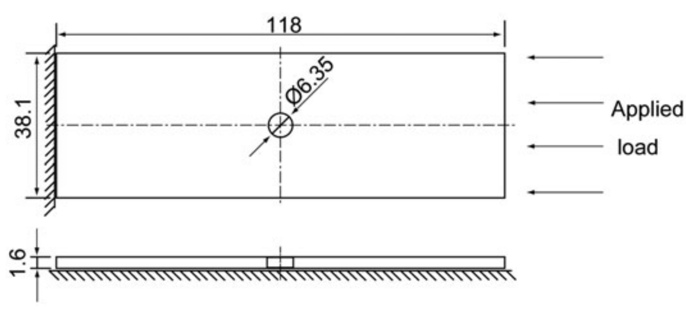

Figure 2. The OHC specimen with stacking sequence $[45/0/-45/90]_{2s}$ and boundary conditions.

Tensile matrix failure

$$\text{If } k_{\mathrm{T,m}} \geq 1,\ \text{then } d_{\mathrm{m}} = 0.99 \tag{8}$$

Compressive matrix failure

$$\text{If } k_{\mathrm{C,m}} \geq 1,\ \text{then } d_{\mathrm{m}} = 0.99 \tag{9}$$

For each loading step, the stress and strain are updated considering the nonlinear shear behavior of the laminates, macro–micro stress conversion, the MMF parameters calculation of the constituents, the damage parameters calculation based on failure indices, and the material properties degradation are implemented using the UMAT written with the Abaqus scripts.

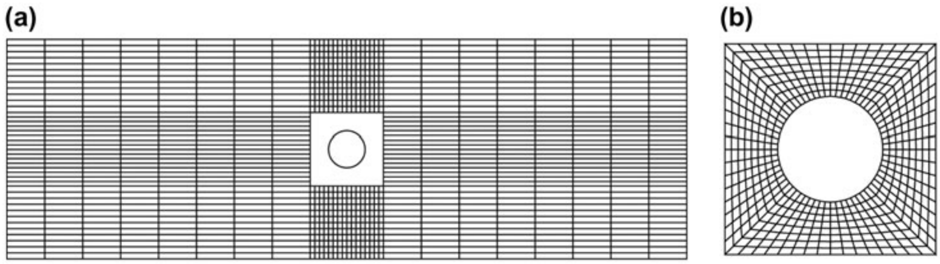

Figure 3. Mesh of the FEM model for the OHC specimen, (a) mesh for the whole model, (b) mesh near the hole.

Table 1. Material properties of the UD laminate for UTS50/E51.

Material properties	Ply	Fiber	Matrix
Fiber volume fraction V_f	0.56	1.0	0.0
Longitudinal modulus E_1 (GPa)	136	240	3.0
Transverse modulus $E_2 = E_3$(GPa)	10	42	3.0
Shear modulus $G_{12} = G_{13}$ (GPa)	4.7	23	1.06
Shear modulus G_{23}(GPa)	3.2	12	1.09
Poisson's ratios $\mu_{12} = \mu_{13}$	0.35	0.33	0.38
Poisson's ratio μ_{23}	0.56	0.71	0.38
Longitudinal coefficient of thermal expansion α_1 (1/k)	-0.34×10^{-6}	-0.87×10^{-6}	6.0×10^{-5}
Transverse coefficient of thermal expansion $\alpha_2 = \alpha_3$ (1/k)	75×10^{-6}	40×10^{-6}	6.0×10^{-5}

Table 2. The uniaxial strengths of the UD laminate for UTS50/E51.

Strength parameters	Average value (MPa)
Longitudinal tensile strength X	2100
Longitudinal compressive strength X'	1932
Transverse tensile strength Y	54
Transverse compressive strength Y'	179
Shear strength S	140

Table 3. The MMF critical parameters of UTS50/E51.

Strength parameters	Values (MPa)
Fiber tensile strength T_f	3710
Fiber compression strength C_f	3430
Matrix tensile strength T_m	155
Matrix compression strength C_m	207

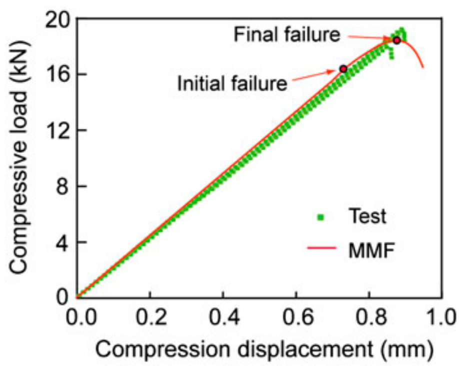

Figure 4. The predicted load-displacement of the OHC structure made of UTS50/E51 laminate with stacking sequence $[45/0/-45/90]_{2s}$ under static compressive loading.

4. Geometry model and material parameters of composites

The OHC structure was made of multidirectional quasi-isotropic laminate with a stacking sequence of $[45/0/-45/90]_{2s}$. The specimen geometry and boundary conditions are shown in Figure 2. The FEM element type is three-dimensional solid elements C3D8R, and the analysis is implemented using Abaqus scripts. Figure 3 shows the mesh of the FEM model for the OHC specimen.

The composite material properties and uniaxial ply strengths used in the demonstrations were obtained from the work of Li et al. [16]. Here, the transverse Young's modulus of the fiber E_{f2} and shear modulus of the fiber G_{f12} are corrected using the finite element analysis and artificial neural networks back-calculate. The material properties

Table 4. Constituents failure modes from initial to final failure based on MMF.

Compression displacement (mm)	45 degree layer		0 degree layer		−45 degree layer		90 degree layer	
	Fiber	Matrix	Fiber	Matrix	Fiber	Matrix	Fiber	Matrix
0.72			●					
0.73		●	●	●		●		
0.74		●	●	●		●		●
0.74–0.89		●	●	●		●		●
>0.89	●	●	●	●	●	●	●	●

Note: ● – Means damage

Table 5. Constituents failure modes from initial to final failure based on Hashin.

Compression displacement (mm)	45 degree layer		0 degree layer		−45 degree layer		90 degree layer	
	Fiber	Matrix	Fiber	Matrix	Fiber	Matrix	Fiber	Matrix
0.43								●
0.43–0.49								●
0.5		●				●		●
0.5–0.56		●				●		●
0.57		●		●		●		●
0.57–0.65		●		●		●		●
0.66		●	●	●		●		●
0.66–0.8		●	●	●		●		●
>0.8	●	●	●	●	●	●	●	●

Note: ● – Means damage.

of the UD laminate for UTS50/51 are listed in Table 1. The uniaxial strengths of the UD laminate for UTS50/51 are listed in Table 2. The MMF critical parameters of UTS50/E51 are shown in Table 3.

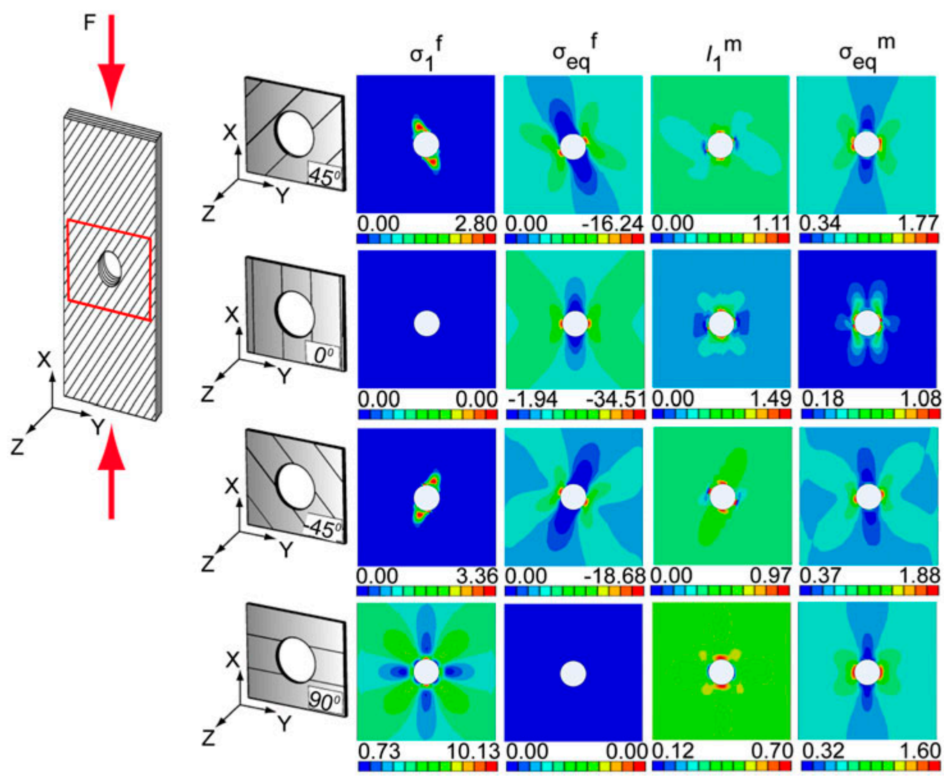

Figure 5. The MMF parameters distribution of first four layer for the initial failure of OHC structure made of UTS50/E51 laminate with stacking sequence $[45/0/{-45}/90]_{2s}$ under static compression (×100 MPa).

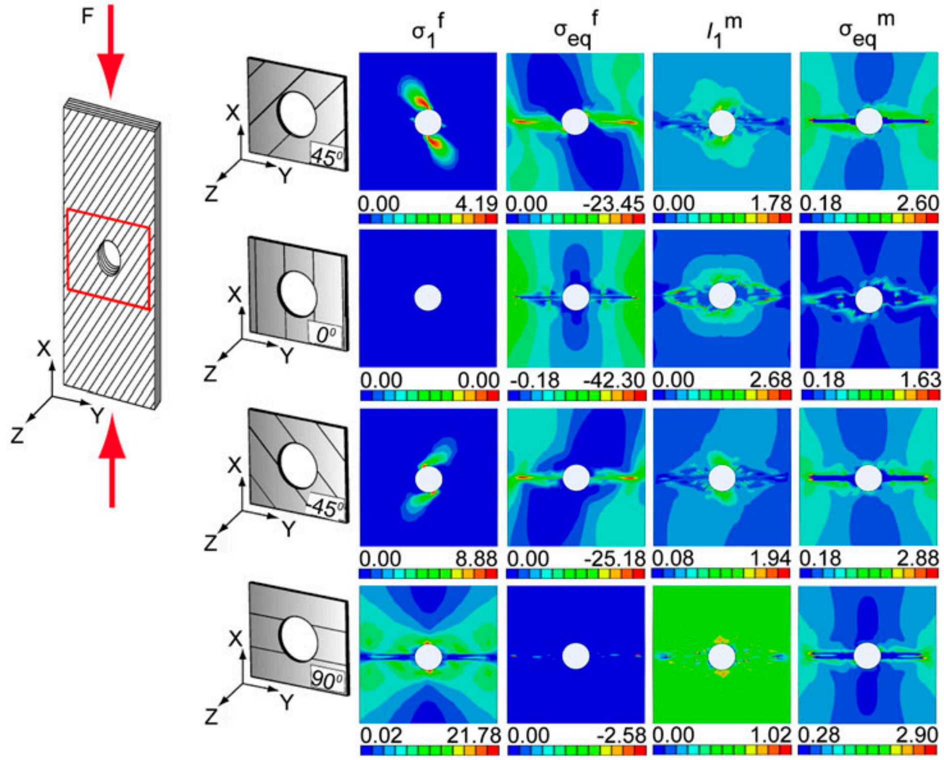

Figure 6. The MMF parameters distribution of first four layer for the final failure of OHC structure made of UTS50/E51 laminate with stacking sequence $[45/0/-45/90]_{2s}$ under static compression (×100 MPa).

5. Results and discussion

The load-displacement curves and damage patterns by the MMF theory approach for the OHC structure bearing the static compressive loading are shown in Figure 4. For comparison, the experimental results of Li et al. [16] are also presented.

From Figure 4, it appears that the MMF theory prediction of the load-displacement curve for the OHC structure appears to be very good with the experimental curve. The predicted ultimate load is reasonably close to peaks of the experimental curves. The ultimate load of OHC structure, obtained from MMF analysis, is 18.4 kN. The relative error is 3.17%.

The constituents' failure modes are identified from the initial failure to the final failure by the MMF failure criteria. At the initial failure, the main failure modes of the OHC structure are the fiber failure of the 0 degree layer. Then matrix failure has formed in the 0 degree layer and the ±45 degree layer. Shortly thereafter at the final failure, matrix failure has formed in every layers and fiber failure only occur in the 0 degree layer, as shown in Table 4.

However, the Hashin theory analysis shows that the initial failure of the OHC structure is triggered by matrix failure in the 90 degree layer, then the matrix failure is found in ±45 degree layer and the 0 degree layer, the fiber failure is detected in the 0 degree layer at last, as shown in Table 5. The static strength of OHC structure,

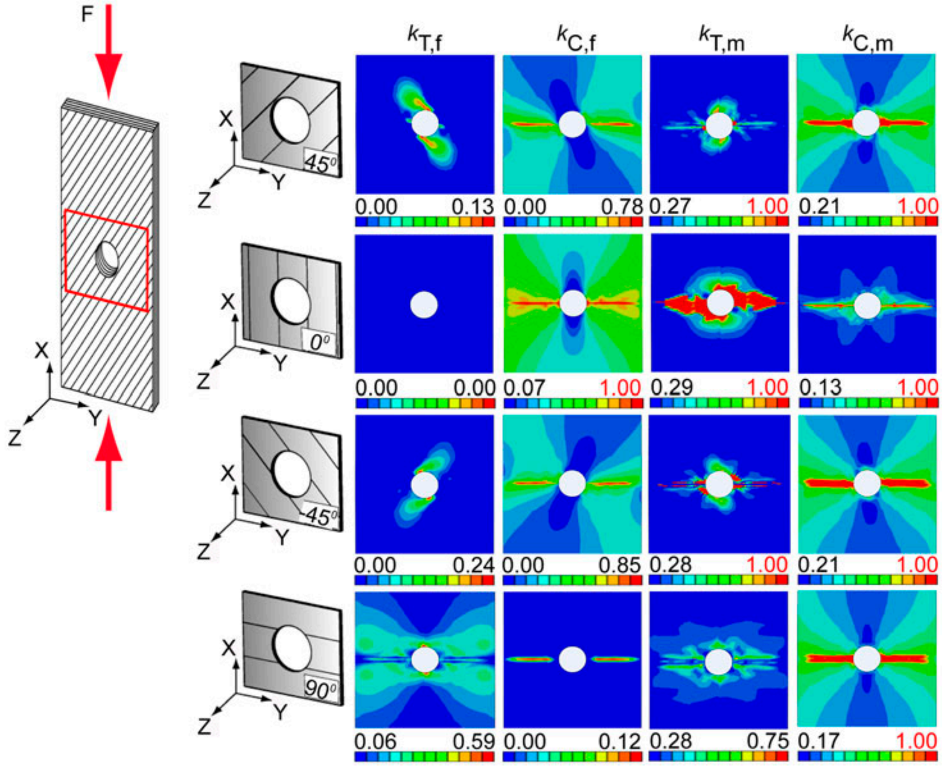

Figure 7. Failure indices distribution of first four layer of OHC structure made of UTS50/E51 laminate with stacking sequence $[45/0/{-45}/90]_{2s}$ under static compression.

obtained from the Hashin theory analysis, is 16.5 kN. The relative error is 12.7%. It means that the approach with the MMF theory provides a more accurate ultimate load prediction. The damage development will be discussed in detail below.

The micro-scale stresses of the constituents (fiber and matrix) of the OHC structure are analyzed using the MMF theory. The distributions of four kinds of the MMF parameters for each layer are plotted. The results of initial failure of the OHC structure for the first four layers are shown in Figure 5. It shows that the distribution of four kinds of the maximum MMF parameters is concentrated around the small hole for each layer, where the failure of OHC structure occurs at edge of layer 0 degrees of the hole in the transverse direction, the MMF parameter σ^f_{eq}, i.e. the maximum compressive stress in the fiber is 3451 MPa, beyond the MMF critical parameters C_f 3430 MPa.

The four kinds of the MMF parameters for the final failure of the OHC structure for the first four layers are shown in Figure 6. It indicates that the linear distribution areas are extended at edge of the hole in perpendicular to the loading direction. The maximum MMF parameters are concentrated at the tip of the linear area, but the MMF parameters out of this area are lower. All cracks in each layer propagate transversely, being perpendicular to the loading direction. This phenomenon is consistent with the experimental observation of Li et al. [16].

The failure indices of all elements for each layer are analyzed in each loading step. The results of final failure of the OHC structure for the first four layers are shown in

Figure 7. For the final failure case, it shows that the constituents failure take place in every layer. The failure of the first, third, and fourth layer are triggered by the matrix failure. The failure of the second layer is triggered by the fiber compressive failure, and the fiber failure also leads to the matrix failure simultaneously. The above analysis shows that the main reason accounting for the OHC structure failure is the fiber compressive failure of 0 degree layer. Damage of the fibers initiates at the edge of the blunt notch and then propagates perpendicular to the loading direction linearly. The matrix failure of the second layer follows the fibers failure, and the actual area of the matrix failure is larger than that of the fiber failure, being caused by the compressive shear.

The real-time monitoring of the failure during test step by step is very difficult. The initial failure of the OHC test was the fiber failure of the 0 degree layer; this phenomenon has been observed experimentally. For the OHC test, the displacement change from the initial failure to the final failure is about 0.1 mm, it is also difficult to capture the failure procedure by stopping the test. The peeling of 45 degree layer near the hole was observed, but the sudden drop was not observed owing to small change of the load, the load-displacement curve of the OHC structure of the quasi-isotropic laminate being almost linear with descending slope until the final failure. The matrix failure of the 45 degree layer does not make an obvious change in the tested load-displacement

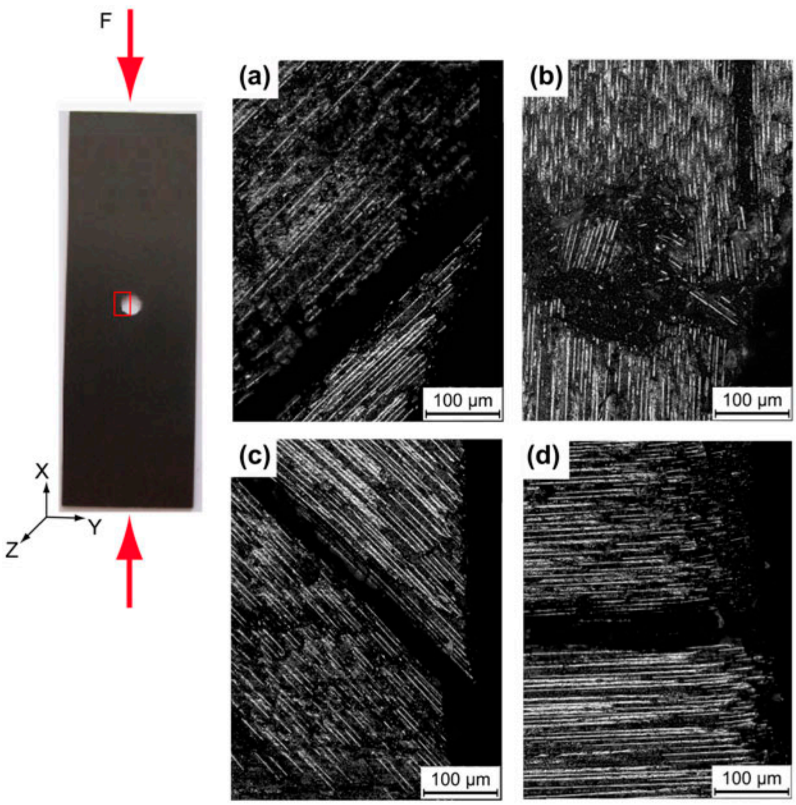

Figure 8. Microscopic fractural surface of first four layers of OHC structure made of UTS50/E51 laminate with stacking sequence $[45/0/{-45}/90]_{2s}$, (a) the 45 degree layer, (b) the 0 degree layer, (c) the −45 degree layer, and (d) the 90 degree layer.

curve. The final failure fractograph near the hole of each layer of OHC structure is observed with optical microscope. In order to observe the inside layer, the surface layers should be removed by grinding. The microscopic fractural surfaces of final failure of the OHC structure for the first four layers are shown in Figure 8. It shows that the failure mechanism of 0 degree layer is fibers kink buckling. While, all the rest failure mechanism of ±45 degree and 90 degree layers are matrix failure. The microscopic observation confirms that OHC structure failures are due to the fibers compressive failure of 0 degree layer. The experimental result and observation validate the accuracy of the predicted results.

6. Conclusions

The method of strength prediction for the CFRP composites structure was established based on the theory of MMF with noninteractive failure criteria and progressive failure analysis. During the process of loading, the constituents' failure was identified by the MMF failure criteria, and then the material properties degradation scheme was evaluated according to the failure modes of constituents and applied for each element to continue the progressive failure analysis for the composite materials. This method can accurately analyze the progressive failure behavior of CFRP composite structures. The UMAT for the micro-scale stress amplification in constituents, failure judgment of the constituents and degradation of ply properties were developed using the Abaqus Fortran scripts, and micro-scale stress of the constituents was visualized for detailed analysis. Prediction of the initial failure, subsequent propagation and final failure, and the ultimate load of OHC structure made of CFRP laminates were achieved based on the MMF theory. The failure mechanism and crack growth process predicted using the MMF theory coincides well with the experiment observation. The predicted ultimate load agrees well with the experimental results, the relative error being 3.17%. Therefore, the MMF theory with noninteractive failure criteria is adequate to be used for the structure design of composite materials.

Funding

This work is supported by National Science Foundation of China and Civil Aviation Administration of China (No. 61079011), and supported by the Fundamental Research Funds for the Central Universities.

References

[1] Icardi U, Locatto S, Longo A. Assessment of recent theories for predicting failure of composite laminates. Appl. Mech. Rev. 2007;60:76–86.
[2] Daniel IM. Failure of composite materials. Strain. 2007;43:4–12.
[3] Saito H, Takeuchi H, Kimpara I. Experimental evaluation of the damage growth restraining in 90° layer of thin-ply CFRP cross-ply laminates. Adv. Compos. Mater. 2012;21:57–66.
[4] Suemasu H, Naito Y, Gozu K, Aoki Y. Damage initiation and growth in composite laminates during open hole compression tests. Adv. Compos. Mater. 2012;21:209–220.
[5] Katoh H, Ishikawa T. Fatigue behavior and lifetime distribution of impact-damaged carbon fiber/toughened epoxy composites under compressive loading. Adv. Compos. Mater. 2013;22:65–78.
[6] Sakai T, Wakayama S, Pérez-Pacheco E, Rodriguez-Laviada J, Rios-Soberanis CR. Damage accumulation behavior of non-crimp fabric-reinforced epoxy composite under static and cyclic tensile loading. Adv. Compos. Mater. 2013;22:281–297.

[7] Herakovich CT. Mechanics of composites: a historical review. Mech. Res. Commun. 2012;41:1–20.
[8] Tsai SW, Wu EM. A general theory of strength for anisotropic materials. J. Compos. Mater. 1971;5:58–80.
[9] Sun CT. Strength analysis of unidirectional composites and laminates. In: Anthony Kelly and Carl Zweben, editors. Comprehensive composite materials. Vol. 1. Oxford: Elsevier; 2000. p. 641–666.
[10] Pinho ST, Iannucci L, Robinson P. Physically-based failure models and criteria for laminated fibre-reinforced composites with emphasis on fibre kinking: part I: development. Composites Part A. 2006;37:63–73.
[11] Pinho ST, Iannucci L, Robinson P. Physically based failure models and criteria for laminated fibre-reinforced composites with emphasis on fibre kinking. part II: FE implementation. Composites Part A. 2006;37:766–777.
[12] Okabe T, Motani T, Nishikawa M, Hashimoto M. Numerical simulation of microscopic damage and strength of fiber-reinforced plastic composites. Adv. Compos. Mater. 2012;21:147–163.
[13] Hashin Z. Failure criteria for unidirectional fiber composites. J. Appl. Mech. 1980;47:58–80.
[14] Puck A, Schürmann H. Failure analysis of FRP laminates by means of physically based phenomenological models. Compos. Sci. Technol. 1998;58:1045–1067.
[15] Ha SK. Micro-mechanical failure theory continuous fiber reinforced composites. Proceedings of the 12th composites durability workshop (CDW-12), St. Maximin, France, ICCM (CD-Rom); 2007.
[16] Li WN, Cai HN, Li C. Static compressive strength prediction of open-hole structure based on non-linear shear behavior and micro-mechanics. Mech. Time-Depend. Mater. 2012;. doi:10.1007/s11043-012-9206-9.
[17] Christensen RM. A Two-property yield, failure (fracture) criterion for homogeneous, isotropic materials. J. Eng. Mater. Technol. 2004;126:45–52.
[18] Cai HN, Miyano Y, Nakada MJ. Long-term fatigue strength prediction of CFRP structure based on micromechanics of failure. J. Compos. Mater. 2008;42:825–830.
[19] Kachanov LM. Rupture time under creep conditions. Int. J. Fract. 1999;97:11–18.
[20] McCarthy CT, O'Higgins RM, Frizzell RM. A cubic spline implementation of non-linear shear behaviour in three-dimensional progressive damage models for composite laminates. Compos. Struct. 2010;92:173–181.